Tokyo Climate Center, Japan Meteorological Agency

TCC News

No. 13 Summer 2008

Contents

Summary of the 2007/2008 La Niña Event

A La Niña event occurred from spring 2007 to spring 2008 for the first time since the 2005/2006 occurrence. In this 2007/2008 event, the minimum value of five-month running mean sea surface temperature (SST) deviations for the NINO.3 region was –1.5˚C, which equaled the record lows of the 1988/1989 and 1998–2000 La Niña events.

1. Outline of the 2007/2008 La Niña event

The Japan Meteorological Agency (JMA) monitors the SST of the NINO.3 region (5°S–5°N, 150°E–90°E), where inter-annual variability is the largest in the equatorial Pacific, to identify El Niño/La Niña events (http://ds.data.jma.go.jp/tcc/tcc/products/elnino/index.html). The five-month running mean value of NINO.3 SST deviation from the latest 30-year sliding mean was equal to or below –0.5°C for 13 consecutive months from April 2007 to April 2008, as shown in Table 1. A La Niña event occurred from spring 2007 to spring 2008, according to JMA's definition of a La Niña event (i.e., the five-month running mean SST deviation for the NINO.3 region is –0.5°C or below for six consecutive months or longer). This was the first La Niña event since the 2005/2006 occurrence, and the 13th such event since 1949 (Table 2).

Table 1 El Niño Monitoring Indices from January 2007 to June 2008
SST values consist of monthly mean sea surface temperatures averaged over the NINO.3 region (5˚S–5˚N, 150˚W–90˚W). SST deviation for the NINO.3 region is defined as the difference between the monthly mean SST and the climatological mean for a sliding 30-year period. Five-month mean values in italics with blue shading indicate levels below –0.5˚C and that a La Niña event is ongoing. Numbers in red indicate SST minima during the 2007/2008 La Niña event.

	2007												2008					
	Jan.	Feb.	Mar.	Apr.	May	Jun.	Jul.	Aug.	Sep.	Oct.	Nov.	Dec.	Jan.	Feb.	Mar.	Apr.	May	Jun.
Monthly mean SST (℃)	26.5	26.4	26.7	26.9	26.4	25.9	24.9	24.0	23.7	23.5	23.5	23.6	24.2	25.0	26.5	27.1	27.0	26.5
SST deviation (℃)	+0.8	0.0	-0.5	-0.5	-0.7	-0.6	-0.8	-1.1	-1.3	-1.5	-1.6	-1.7	-1.5	-1.4	-0.6	-0.3	-0.1	0.0
5-month mean (℃)	+0.5	+0.2	-0.2	*-0.5*	*-0.6*	*-0.7*	*-0.9*	*-1.1*	*-1.3*	*-1.4*	*-1.5*	*-1.5*	*-1.4*	*-1.1*	*-0.8*	*-0.5*	-	-
SOI	-0.6	-0.1	+0.1	+0.1	-0.2	+0.5	-0.5	+0.4	+0.1	+0.7	+0.8	+1.6	+1.4	+1.8	+1.3	+0.6	-0.2	+0.5

Table 2 List of historical La Niña events since 1949 based on JMA's definition along with duration seasons/months and minimum values of five-month/monthly mean NINO.3 SST
Numbers in red indicate record lengths in terms of duration and minimum records in terms of NINO.3 SST.

Historical La Niña events		Duration		Index of NINO.3 peak	
Sequence number from 1949	Periods of La Niña events (Boreal season and year)	seasons	months	5-month mean (˚C)	monthly mean (˚C)
1	Summer 1949 — Summer 1950	5	13	- 1.2	- 1.4
2	Spring 1954 — Winter 1955 /56	8	23	- 1.2	- 1.7
3	Spring 1964 — Winter 1964 /65	4	10	- 1.0	- 1.2
4	Autumn 1967 — Spring 1968	3	8	- 0.9	- 1.3
5	Spring 1970 — Winter 1971 /72	8	20	- 1.1	- 1.5
6	Spring 1973 — Spring 1974	4	10	- 1.2	- 1.5
7	Spring 1975 — Spring 1976	5	12	- 1.0	- 1.3
8	Spring 1984 — Autumn 1985	6	15	- 0.9	- 1.1
9	Spring 1988 — Spring 1989	5	13	- 1.5	- 1.8
10	Summer 1995 — Winter 1995 /96	3	8	- 0.8	- 1.0
11	Summer 1998 — Spring 2000	8	21	- 1.5	- 1.8
12	Autumn 2005 — Spring 2006	3	6	- 0.8	- 1.2
13	Spring 2007 — Spring 2008	5	13	- 1.5	- 1.7

The 2007/2008 La Niña event was a typical one that developed from spring, continued for about a year and decayed in the spring of the following year. In this event, the minimum value of the five-month running mean NINO.3 SST deviation was –1.5˚C, which equaled the record lows of the 1988/1989 and 1998–2000 La Niña events. The minimum value of monthly mean NINO.3 SST deviation was –1.7˚C, which is the joint third largest along with the 1954–1956 occurrence, after the –1.8˚C value of the 1988/1989 and 1998–2000 La Niña events.

2. Progress of the 2007/2008 La Niña event

Figure 1 shows a time-longitude cross section of five-day averaged SST anomalies along the equator in the Pacific Ocean. In January 2007, positive SST anomalies were widely found in the equatorial Pacific. In March 2007, remarkably negative SST anomalies appeared east of 150˚W in the NINO.3 region. An SST anomaly pattern typical of those seen during La Niña events (i.e., negative in the eastern equatorial Pacific and positive in the western part) remained until August 2007. In September 2007, remarkably negative SST anomalies expanded to the west of the date line, widely covering the area from the central equatorial Pacific to its eastern part. Thereafter, remarkably negative SST anomalies gradually extended westward, and both NINO.3 and NINO.4 SSTs became remarkably below normal in October 2007. In February 2008, the minimum values of negative SST anomalies in this event were widely found from the date line to 120˚W. On the other hand, after January 2008, positive SST anomalies expanded gradually from the coast of South America to the eastern equatorial Pacific. In March 2008, remarkably positive SST anomalies were found east of 110˚W in the equatorial Pacific. The negative SST anomalies from the central to the eastern equatorial Pacific gradually shrank, and negative anomalies of less than –0.5˚C were found only around the date line in June 2008.

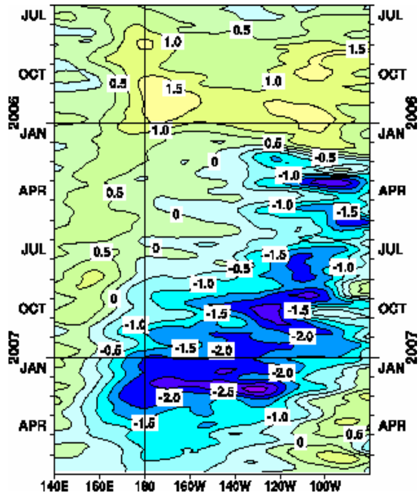

Figure 1 Time-longitude cross section of SST anomalies along the equator in the Pacific Ocean
The base period for the normal is 1971–2000.

The processes of La Niña events are classified into the onset phase, the peak phase, the mature phase and the following phase, after Rasmusson and Carpenter (1982) (Figure 2).

During the onset phase from October to December (OND) 2006, positive anomalies were remarkable from the central to the eastern equatorial Pacific (Figure 2a). In the depth-longitude cross section of three-month averaged temperatures and anomalies (Figure 2e), positive anomalies in the eastern equatorial Pacific and negative anomalies in the western part were remarkable, indicating temporal El Niño-like features.

During the peak phase from April to June (AMJ) 2007, when the La Niña event began to develop, negative SST anomalies expanded over the eastern equatorial Pacific, and monthly mean NINO.3 SST deviation was from –0.5˚C to –0.7˚C (Table 1). Meanwhile, during the same period, positive SST anomalies were found from the western to the central equatorial Pacific (Figure 2b). In upper-ocean temperatures along the equatorial Pacific, colder waters that were found in the western part during the onset phase migrated to the eastern part, resulting in remarkably negative temperature anomalies in the eastern part and near-normal ones in the western part (Figure 2f). During the mature phase from October to December 2007, negative SST anomalies expanded to the central and western equatorial Pacific, covering most of the equatorial Pacific except for the

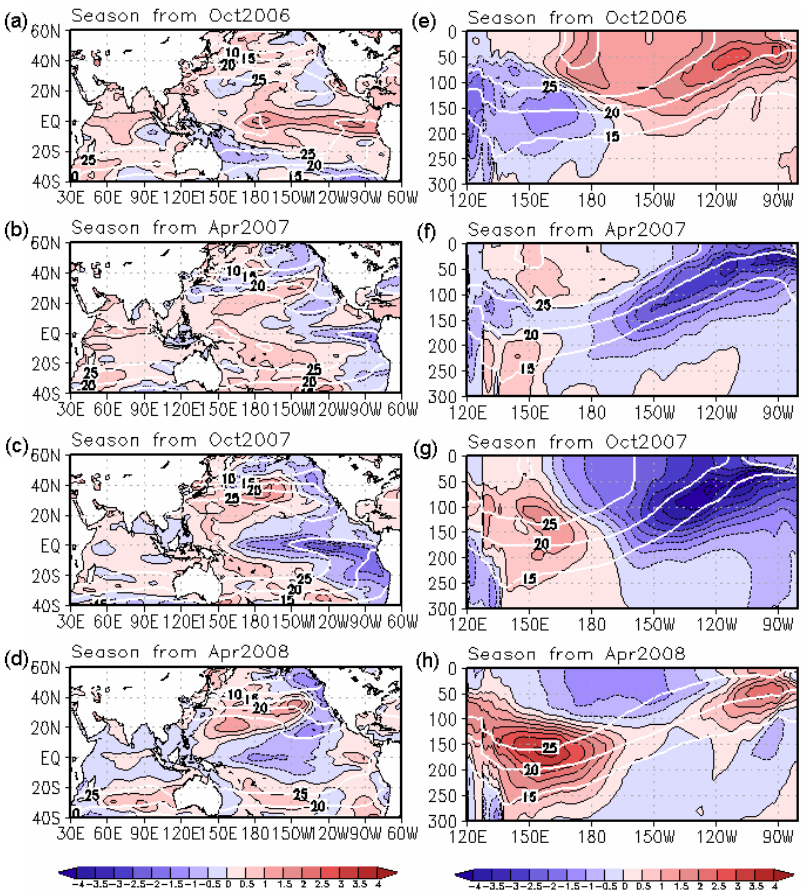

Figure 2 Three-month mean sea surface temperatures (SSTs) and anomalies in the Pacific and Indian Oceans (left) and depth-longitude cross sections of three-month mean temperatures and anomalies upper 300 m along the equatorial Pacific (right)
White contours indicate SSTs/temperatures at intervals of 5˚C. The top panels (a and e) show the onset phase during OND 2006, the second ones down (b and f) show the peak phase during AMJ 2007, the third panels (c and g) show the mature phase during OND 2007, and the bottom ones (d and h) show the following phase during AMJ 2008 of La Niña events. These phase names are those used by Rasmusson and Carpenter (1982).

westernmost part (Figure 2c). During this period, the east-west contrast of upper-ocean temperature anomalies (i.e., negative in the eastern part and positive in western part) was remarkable in the equatorial Pacific.

During the following phase from April to June 2008, positive SST anomalies appeared in the eastern equatorial Pacific, and negative SST anomalies were found only in the central part (Figure 2d). In the depth-longitude cross section along the equatorial Pacific, positive temperature anomalies became remarkable in the western and eastern parts, and positive anomalies along the thermocline depth indicated deepening (Figure 2h). During this phase, negative SST anomalies in the central equatorial Pacific shrank and weakened, resulting in the termination of the 2007/2008 La Niña event in spring 2008.

3. Comparison with other historical events

We compared the progress of the 2007/2008 La Niña event with other historical occurrences of the phenomenon. Figure 3 shows time series composites of three-month running mean SST deviations averaged over the NINO.3 and NINO.4 regions for historical La Niña events since 1949.

In the developing process (i.e., the starting year) of the 2007/2008 La Niña event, SST deviation in the NINO.3 region rapidly decreased from winter to early spring, and a slowdown of the decrease was found from spring to summer. On the other hand, in 1970 and 1988, NINO.3 SST deviations constantly fell and reach their minima during summer. In 2007, NINO.3 SST deviation rapidly fell again from summer, and reached its minimum from autumn to winter (Figure 3a). In the NINO.4 region for the 2007/2008 event, the reduction of SST deviation during spring and summer was slower than that in NINO.3, and SST was near normal in July. SST deviation in NINO.4 decreased rapidly in autumn, and reached its minimum in late winter. The minimum in NINO.4 was found three months later than that in NINO.3. The SST deviation in NINO.4 for 2007 reached its minimum later than those for 1988 and 1998, but the minimum for 2007 had almost the same magnitude as those for 1988 and 1998 (Figure 3b).

In the decaying process (i.e., the finishing year) of the 2007/2008 La Niña events, the SST deviation in NINO.3 rose rapidly after its minimum from late autumn to early winter, and returned to normal with almost the same timing as in spring 1989 and 2000 (Figure 3c). On the other hand, the minimum SST deviation of NINO.4 in the 2007/2008 event was found later than that of the 1988/1989 event. The SST deviation of NINO.4 began to rise from the spring of 2008. Due to the larger magnitude and later timing of the minimum of NINO.4 deviation in the 2007/2008 event, the NINO.4 SST was still below normal in June 2008 (Figure 3d).

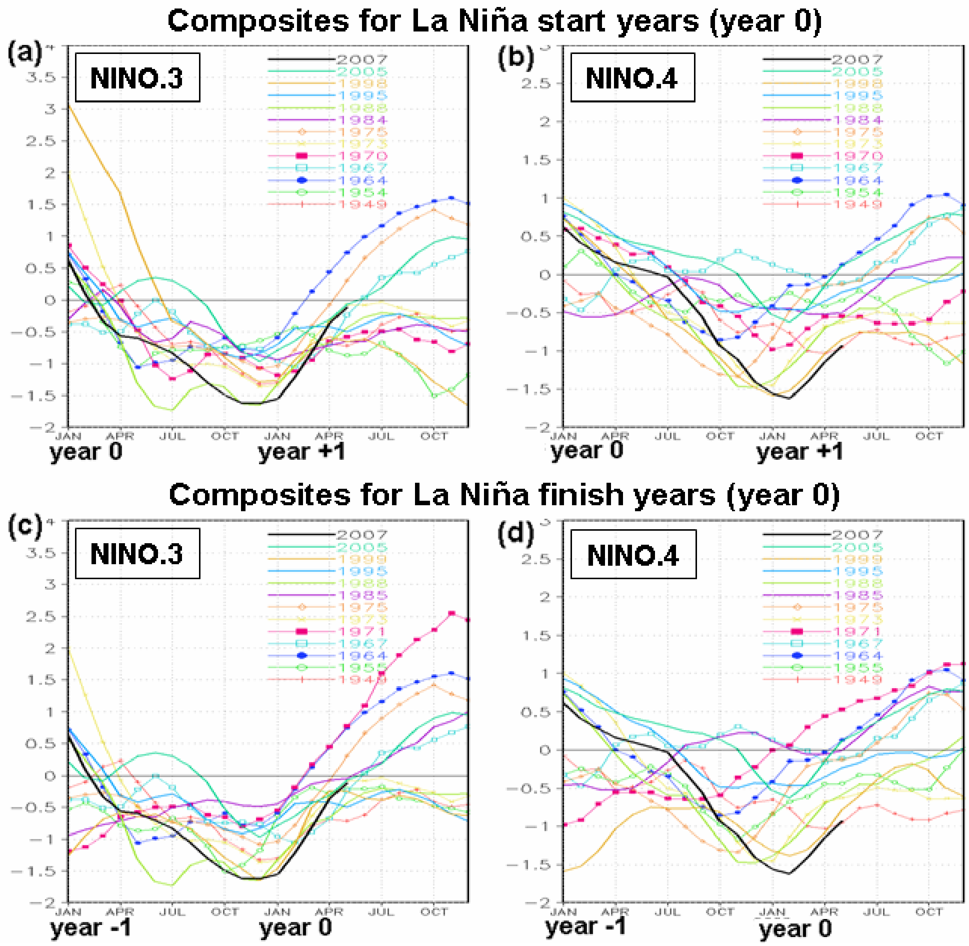

Figure 3 Time series composites of three-month running mean sea surface temperature (SST) deviations averaged over the NINO.3 and NINO.4 regions for historical La Niña events
The upper panels (a and b) show composites for event-starting years, and the lower ones (c and d) show those for event-finishing years. The panels on the left (a and c) show SST composites for the NINO.3 region, and those on the right (b and d) show composites for the NINO.4 region. Normal values are taken as the latest 30-year sliding mean SSTs to remove long-term trends. **Year 0** in the upper panels represents the year that the La Niña event began and **Year+1** means the following year. The La Niña years are 1949, 1954, 1964, 1967, 1970, 1973, 1975, 1984, 1988, 1995, 1998, 2005 and 2007. Meanwhile **Year 0** in the lower panels represents the year that the La Niña event ended and **Year-1** means the previous year.

4. Impact on climate in Japan and around the world

During the 2007/2008 La Niña event, several significant climate anomalies were observed around the world.

In South America, temperatures were lower than normal in southern parts from May to August 2007 and along the Pacific coast from September 2007 to February 2008. Drier conditions were found in northern parts. In North America, warmer and drier conditions appeared in the eastern USA during August 2007. Temperatures were warmer than normal in the southern USA and cooler than normal along the Pacific coast during winter of 2007/2008. In Australia, wetter conditions were found in northern parts from June to August, while drier conditions were found in eastern parts from December 2007 to February 2008. Around the islands of Indonesia, wetter conditions were found from August to September. In Japan, warmer conditions were found from August to September 2007.

Some of the above-mentioned climate anomalies are consistent with those statistically seen during La Niña events (http://ds.data.jma.go.jp/tcc/tcc/products/climate/ENSO/shade/shadela.html).

Reference:

Rasmusson, E. M. and T. H. Carpenter 1982: Variations in Tropical Sea Surface Temperature and Surface Wind Fields Associated with the Southern Oscillation/El Niño. *Mon. Wea. Rev.*, **110**, 354–384.

(Ikuo Yoshikawa, Climate Prediction Division)

Summary of Yellow Sand over Japan in 2008

The number of days when any meteorological station in Japan observed yellow sand, or Aeolian dust, from January to May 2008 was 10, which was the smallest since 1987. Yellow sand was widely observed throughout the country except northern Japan on 3 March, but was subsequently observed only a few times, mainly in western Japan.

JMA carries out observation of the phenomenon at 85 meteorological stations. Yellow sand observed from 2 to 4 March originated from the Gobi Desert on 29 February and spread over Japan along with a cyclone. This event was also detected in MTSAT's infrared differential imagery. In addition, JMA's operational numerical dust model (Model of Aerosol Species In the Global Atmosphere: MASINGAR) successfully forecasted the emission and transportation of yellow sand as early as 28 February.

Since 27 February, a JMA web page providing Aeolian dust information has provided current observation and prediction updates on yellow sand using different colors to indicate its concentration (Figures 4 and 5). (URL: http://www.jma.go.jp/en/kosa/index.html)

From 1 January to 31 May 2008, the number of days when any meteorological station observed yellow sand was 10, which was the smallest since 1987 (Figure 6).

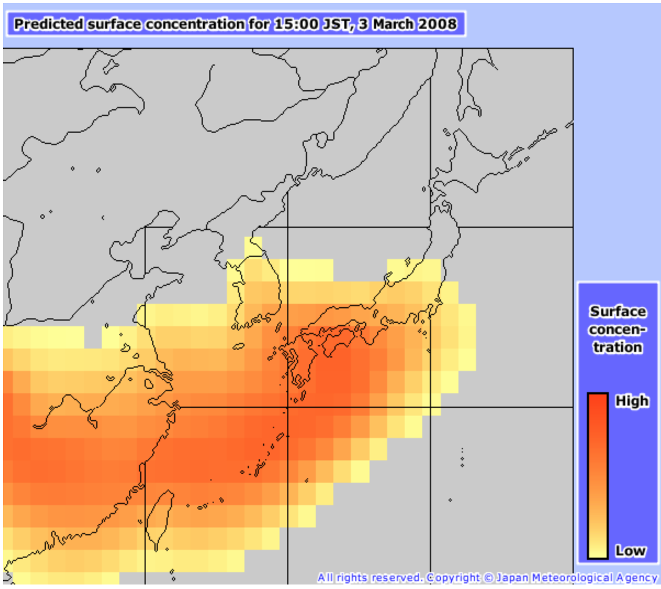

Figure 5 Distribution of predicted concentrations of yellow sand at a level of 0–1 km from the surface for 1.25 x 1.25 degree grid areas

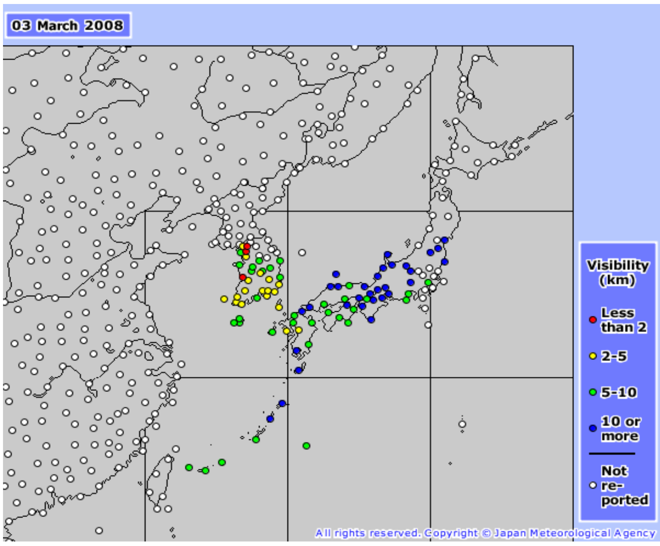

Figure 4 Stations observing aeolian dust or local sand/dust haze during the day
Colors indicate the lowest visibilities observed at these stations.

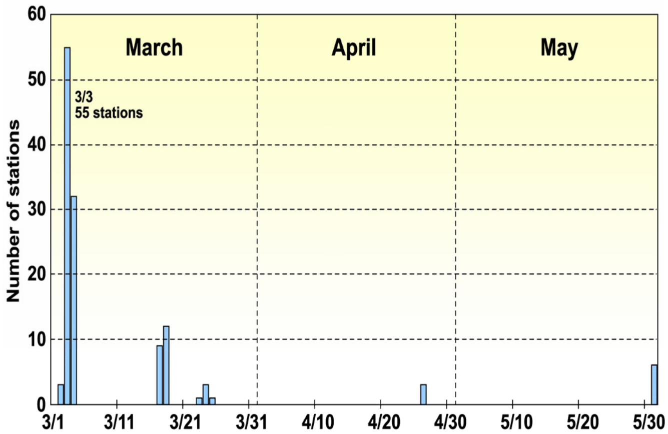

Figure 6 Daily number of meteorological stations that observed yellow sand from 1 March to 31 May 2008 (total number of meteorological stations: 85)
Yellow sand was not observed at any stations from January to February.

The total daily number of meteorological stations that observed the phenomenon in 2008 was 125, which was also the smallest since 1997 (Figure 7). Of special interest is that the total number of days when yellow sand was observed in April was only one, which was far below the normal value of 7.9.

Monthly CLIMAT data show heavy precipitation in northeastern parts of China in April and light precipitation around the Gobi Desert from April to May. Moreover, the Taklimakan Desert experienced light precipitation from March to May according to CLIMAT data averaged over three months (Figure 8). According to SYNOP reports, the number of sandstorm and dust events around the Gobi Desert (95–115°E, 35–50°N) increased by about 25% compared to the previous year, suggesting a more frequent occurrence of yellow sand.

One possible cause of decreased observation of the phenomenon in Japan is that yellow sand rarely blew over the country, or did not reach ground level even if it was present.

Analysis of atmospheric circulation from March to May indicates that the activity of cyclones was weaker than normal around Japan and prevailing westerlies in the middle and upper troposphere did not meander. It is presumed from this circulation pattern that the inflow of yellow sand along with cyclones into Japan was reduced, and that the phenomenon moved zonally from the generation region to the north of the country.

(Atsuya Kinoshita, Atmospheric Environment Division)

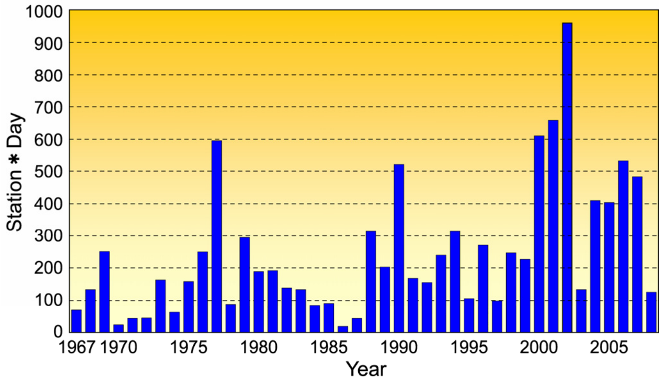

Figure 7 Annual total daily numbers of meteorological stations observing yellow sand from 1967 to 2008

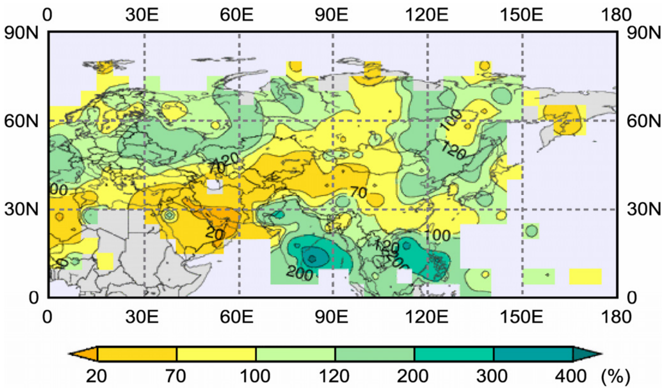

Figure 8 Three-month mean precipitation ratio from March to May 2008 according to CLIMAT data
The Gobi Desert and the Taklimakan Desert experienced light precipitation.

Sea Ice in the Sea of Okhotsk for the 2007/2008 Winter Season

The sea ice extent in the Sea of Okhotsk was smaller than normal for almost all the 2008 sea ice season (from December 2007 to May 2008) (Figure 9). It reached its seasonal maximum of 110.69 x 10^4 km^2 on 10 February, exceeding the highest value for the previous season (Figures 9 and 10). The accumulated sea ice extent was smaller than the previous season (Figure 11), and its ratio to the normal (the 1971–2000 average) was 80%.

Figure 11 shows overall trends for the period from 1971 to 2008. The maximum sea ice extent has fallen by about 15% of the area of the Sea of Okhotsk over approximately the past 40 years. However, sea ice in the Sea of Okhotsk is first-year ice (i.e., ice of not more than one winter's growth), and its interannual extent varies dramatically. As an example, the maximum sea ice extent was 55% of the area of the Sea of Okhotsk in 1984, while it covered almost the entire sea in 2001. Small changes in meteorological and oceanographic forcing could result in significant changes in the extent and state of the sea ice cover.

(Keiji Hamada, Office of Marine Prediction)

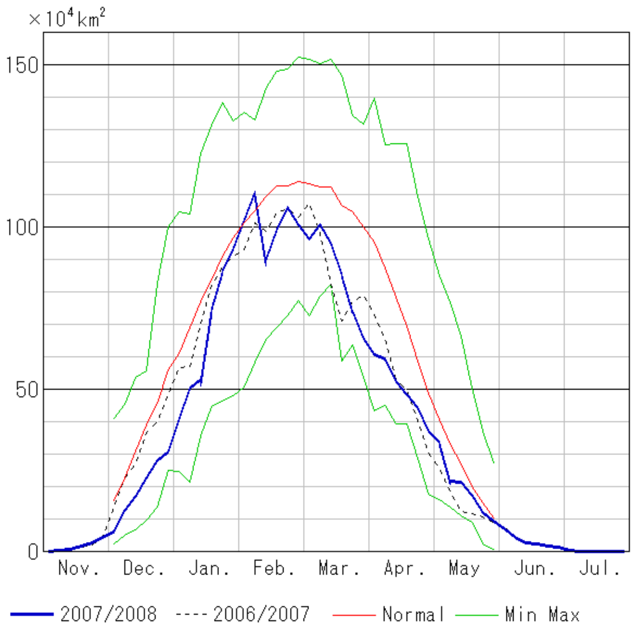

Figure 9 Variations in the five-day mean sea ice extent in the Sea of Okhotsk from November 2007 to July 2008

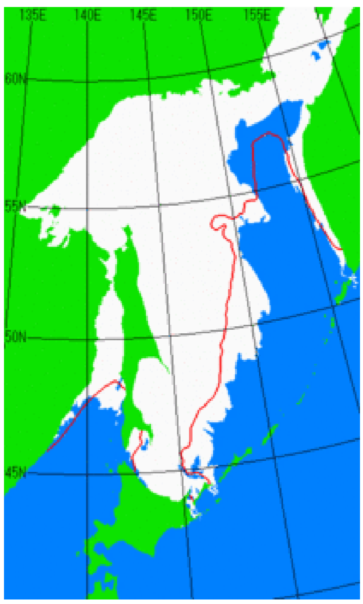

Figure 10 Sea ice conditions for 10 February 2008
The white area shows the observed sea ice extent, and the red line indicates the normal sea ice extent (1971–2000).

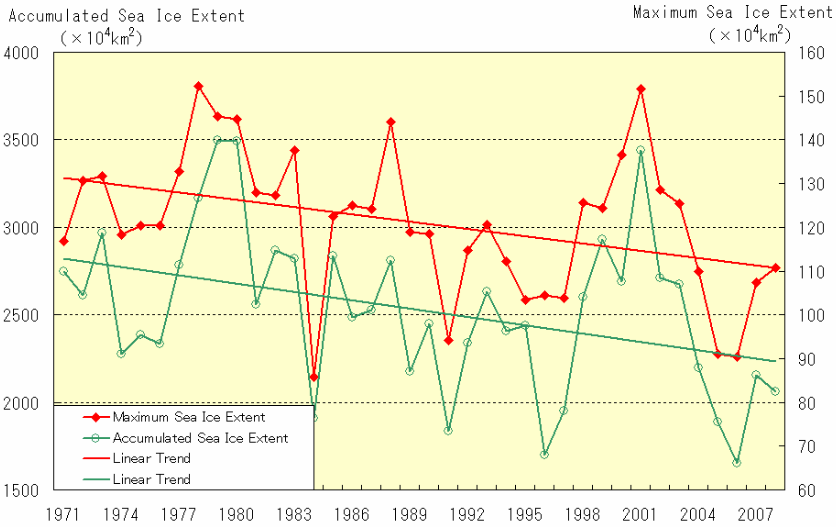

Figure 11 Interannual variations in the maximum sea ice extent (red lines) and accumulated sea ice extent (green lines) in the Sea of Okhotsk from 1971 to 2008
Accumulated sea ice extent: the sum of all five-day sea ice extent values from December of the previous year to May.

Atmospheric Circulation Anomalies behind US Midwest Flooding in June 2008

Introduction

Severe storms battered the Midwest of the USA in early June. According to surface synoptic observations (SYNOP), 10-day precipitation amounts from 1 to 10 June reached 100–230 mm (Figure 12) in the Midwest, a level 3–11 times heavier than the average monthly precipitation. The heavy rainfall and resulting floods along the Mississippi caused serious damage to social and agricultural properties, especially in Iowa and Wisconsin. Summarized below are the characteristics of the large-scale atmospheric circulation anomalies behind the heavy rainfall of early June 2008.

Upper troposphere circulation

Figure 13 shows 250-hPa-level geopotential heights and their anomalies, along with wave activity fluxes derived from 10-day mean height anomalies from 1 to 10 June 2008. Wave activity fluxes indicate the group velocity of a Rossby wave, and are a useful diagnostic tool in illustrating the energy propagation of such waves (Takaya and Nakamura, 2001). In the upper troposphere, a trough in the western US and a ridge in the eastern US developed in association with the energy propagation of a quasi-stationary Rossby wave. This trough involved upper-tropospheric cold air.

The upper-tropospheric jet stream was much stronger than normal from the northeastern Pacific to the western US (Figure 14). In the western US, the jet stream was displaced well south of its normal position due to a developed upper trough. The southwesterly jet over the Midwest suggests that upward motion could have occurred in this area. The strong vertical shear of westerly winds observed in the western US may have represented a favorable atmospheric condition for the development of baroclinic disturbances. In June, synoptic disturbance activity was enhanced from the northeastern Pacific to the Midwest (not shown in the figures).

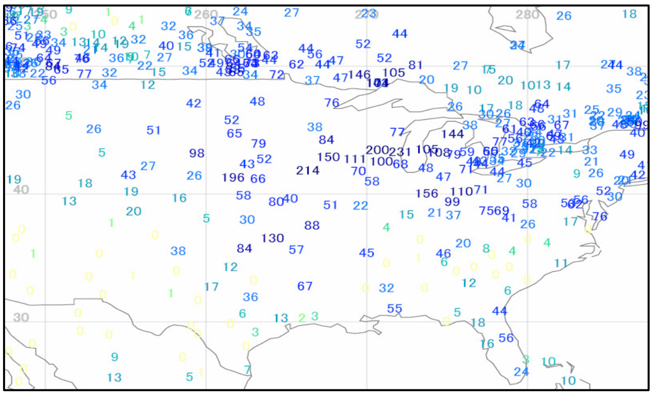

Figure 12 Ten-day precipitation amounts in North America from 1 to 10 June 2008
Precipitation amounts are based on surface synoptic observations (SYNOP).

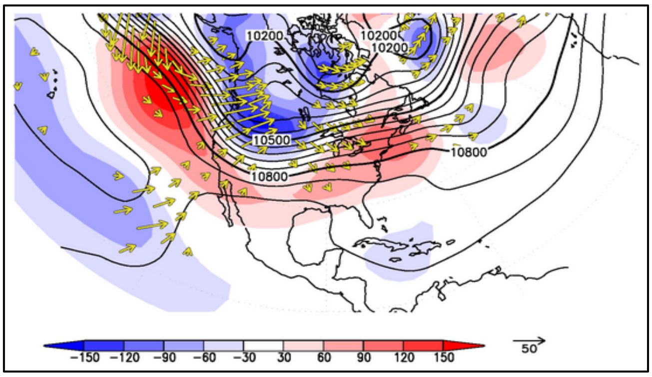

Figure 13 Ten-day mean 250-hPa geopotential heights (contours, unit: m) and their anomalies (colored areas, unit: m), and wave activity fluxes (vectors, unit: m^2/s^2) from 1 to 10 June 2008

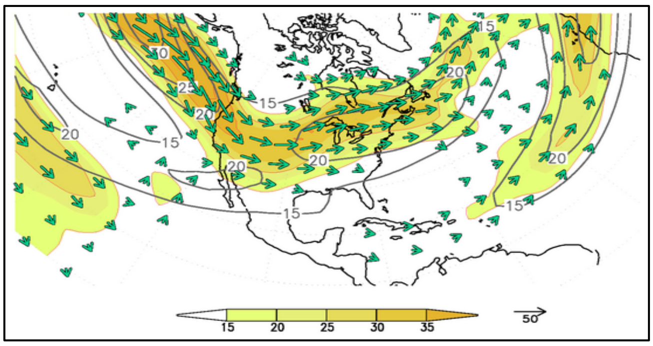

Figure 14 Ten-day mean 200-hPa wind (vectors) and zonal wind speeds (colored areas, unit: m/s) from 1 to 10 June 2008
Gray contours indicate the climatological mean of 200-hPa zonal wind speeds in the same period (unit: m/s).

Lower troposphere circulation

In the lower troposphere, southwesterly winds were stronger than normal from the Bay of Mexico to the Midwest along the edge of the Atlantic subtropical high-pressure system. This flow led to warm air advection in the eastern US (not shown in the figures). A frontal zone in the lower troposphere formed around the Midwest between this warm air mass and a cold air mass in the western US with the upper cold trough mentioned above.

Moreover, the flow from the Bay of Mexico induced anomalous water vapor fluxes. Figure 15 illustrates water vapor fluxes and their divergence at 850-hPa level in early June. The panel on the left shows the 10-day average from 1 to 10 June 2008, while that on the right shows flux deviations and divergence from the normal in the same period. These panels reveal that northward/northeastward water vapor fluxes from the coastal area to the central US were stronger than normal in the lower troposphere. This large flow of atmospheric moisture moved from the Bay of Mexico into the central and eastern US, and a strong convergence of the water vapor fluxes was observed in the Midwest. This excessive supply of water vapor to the Midwest may have been one of the major contributing factors to the heavy rainfall in the area.

Possible effect of SST anomalies

Similar characteristics of atmospheric circulation were found in the case of the Great Flood of summer 1993 (Trenberth and Guillemot, 1996). In that year, sea surface temperature (SST) anomalies in the tropical Pacific showed an El Niño-like structure, while in June 2008 they had a La Niña-like structure. In late May 2008, however, positive SST anomalies were observed around the eastern tropical Pacific and the Caribbean Sea where convective activities were enhanced. The warm SST and active convection may have played an important role in supplying water vapor to the atmosphere in and around the Bay of Mexico.

Summary

From the diagnostic analysis described above, many contributing factors to the heavy rainfall in the Midwest were found in early June. The major influences that may have induced this rainfall are summarized in the schematic diagram in Figure 16. First, an upper-tropospheric trough and an associated southwardly-shifted jet stream created favorable atmospheric conditions for the development of disturbances. These upper-atmospheric conditions persisted during early June in association with the energy propagation of a quasi-stationary Rossby wave. Secondly, warm and moist air flowing along the edge of the Atlantic subtropical high-pressure system formed a strong frontal zone in the lower troposphere and led to an excessive supply of water vapor and its convergence in the Midwest. This may have been one of the major contributing factors to the heavy rainfall in this area. Lastly, warm SST anomalies from the eastern tropical Pacific to the Caribbean Sea and enhanced convective activities may have played a role in supplying water vapor to the atmosphere.

References

Trenberth, K. E., and C. J. Guillemot, 1996: Physical processes involved in the 1988 drought and 1993 flood in North America. *J. Clim.*, **9**, 1288-1298.

Takaya, K., and H. Nakamura, 2001: A formation of a phase-independent wave-activity flux for stationary and migratory quasigeostrophic eddies on a zonally varying basic flow. *J. Atmos. Sci.*, **58**, 608-627.

(Atsushi Goto, Climate Prediction Division)

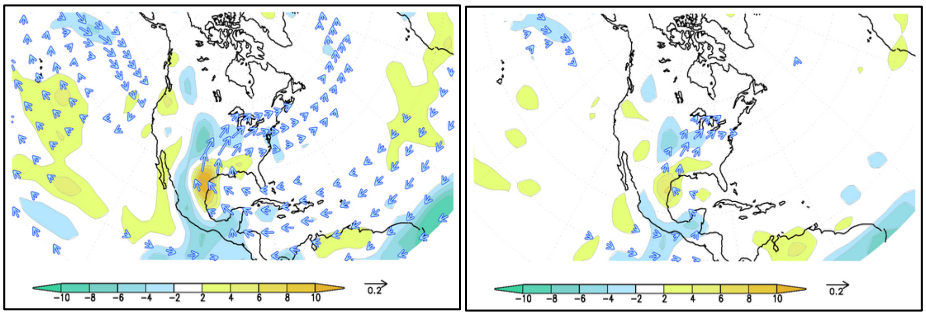

Figure 15 Ten-day mean water vapor fluxes (vectors, unit: kg/kg·m/s) and their divergence (colored areas, unit: 10^{-8}kg/kg/s) at 850-hPa level from 1 to 10 June 2008 (left); the panel on the right shows the same situation as the one on the left, but for deviations from their climatological means in the same period.

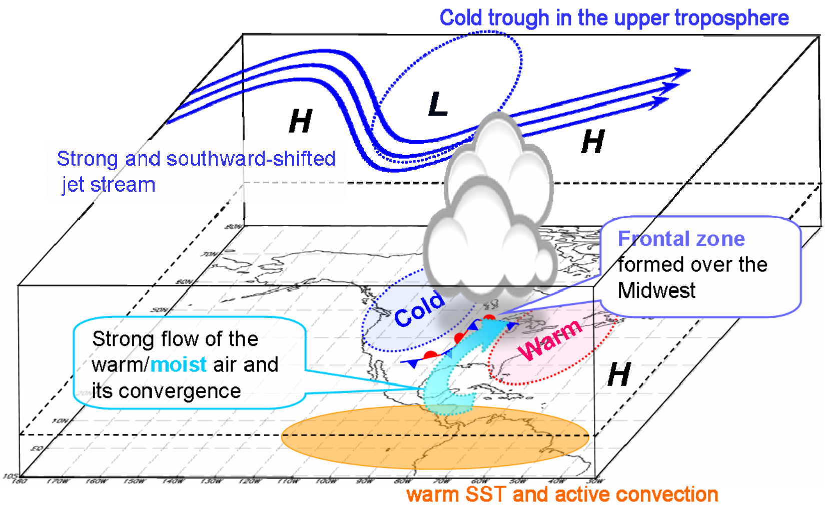

Figure 16 Schematic diagram of atmospheric circulation anomalies observed in early June
This shows possible factors contributing to the heavy rainfall in the Midwest.

WMO Working Group on Climate-Related Matters for Regional Association II (WGCRM RA II)

A meeting of the Working Group on Climate-Related Matters (WGCRM) for Regional Association II (RA II) of the World Meteorological Organization (WMO) took place at the Japan Meteorological Agency (JMA) headquarters in Tokyo, Japan, from 7–8 August 2008. The meeting was attended by seven members of the Working Group from China, India, the Islamic Republic of Iran, Japan, the Republic of Korea and the Russian Federation, and two from the WMO Secretariat. As Dr. Zheng Guoguang, Chair of the WGCRM, was unable to attend the meeting, it was chaired by Dr. Koichi Kurihara of JMA, Vice-Chair of the WGCRM, at the Chair's request.

At the opening ceremony, Dr. Tetsu Hiraki, Director-General of JMA, welcomed the participants on behalf of JMA. He recalled that significant progress has been made in climate-related activities in RA II, particularly in the development of the Regional Climate Center (RCC) Network's activities.

The meeting reviewed the implementation of climate-related activities in RA II including the development of the RCC Network in the region. The meeting also considered future plans for the RCC Network and agreed to further develop cooperative relationship among Members.

A report of the meeting will be submitted to the President of RA II by the Chair of the WGCRM.

(Kumi Hayashi, Climate Prediction Division)

Hands-on Training for Climate Data Communication and Applications at TCC

JMA's Tokyo Climate Center (TCC) ran a hands-on training course on climate data communication and applications from 13 July to 2 August 2008 at the request of the Malaysian Meteorological Department (MMD). The three-week course was attended by Mr. Mohd Sani Bin Saayon and Ms. Nik Noorhayati Binti Nik Abdul Majid from the Climate Section of MMD.

In the training, the participants learned the use of Linux machines, data processing for GRIB and GRIB2 and visualization of climate-related data and products.

Another hands-on training course for climate forecasting and its applications will be held in September this year with the participation of another two officers from MMD.

(Kumi Hayashi, Climate Prediction Division)

Any comments or inquiries on this newsletter and/or the TCC website would be much appreciated. Please e-mail to: tcc@climar.kishou.go.jp

(Chief Editor: Kumi Hayashi)

Tokyo Climate Center (TCC), Climate Prediction Division, JMA
Address: 1-3-4 Otemachi, Chiyoda-ku, Tokyo 100-8122, Japan
TCC website: http://ds.data.jma.go.jp/tcc/tcc/index.html